One-step solid-state pyrolysis of bio-wastes to synthesize multi-hierarchical porous carbon for ultra-long life supercapacitors

Min Fu,[a] Jintao Huang,[b,c*] Simin Feng,[d] Tianyi Zhang,[e] Peng-Cheng Qian,[f,*] Wai-Yeung Wong[c,*]

[a] College of Chemical and Biological Engineering, Shandong University of Science and Technology, Qingdao 266590, China

[b] Department of Polymeric Materials and Engineering, School of Materials and Energy, Guangdong University of Technology, Guangzhou, 510006, China

[c] Department of Applied Biology and Chemical Technology and Research Institute for Smart Energy, The Hong Kong Polytechnic University, Hung Hom, Hong Kong, China

[d] i-Lab, Key Laboratory of Multifunctional Nanomaterials and Smart Systems, Suzhou Institute of Nano-Tech and Nano-Bionics, Chinese Academy of Sciences, Suzhou, 215123, China

[e] Department of Materials Science and Engineering, The Pennsylvania State University, University Park, PA 16802, USA

[f] Key Laboratory of Environmental Functional Materials Technology and Application of Wenzhou City, Institute of New Materials & Industry, College of Chemistry & Materials Engineering, Wenzhou University, Wenzhou 325035, China

Corresponding authors: polyhjt@163.com (Jintao Huang), wai-yeung.wong@polyu.edu.hk (Wai-Yeung Wong), qpc@wzu.edu.cn (Peng-Cheng Qian)

ABSTRACT

Porous carbon is highly desired in supercapacitor electrodes due to high specific surface area, ample pore size and superior electrochemical stability. Yet developing a

general and simple synthetic method to prepare porous carbon remains challenging. Meanwhile, recycling waste to obtain high value-added materials is an effective way to solve environmental pollution and resource shortage problems. Herein, a general one-step solid-state pyrolysis method is developed to synthesize multi-hierarchical porous carbon using bio-wastes as precursors and potassium ferrate as pore-forming agent. This method is superior to the traditional two-step or multi-step method due to its simple procedures, low cost, little pollution and time-saving features. Multiple pore-forming effect derived from potassium ferrate is responsible for such multi-hierarchical porous structure. The resulting porous carbon is used to fabricate symmetrical supercapacitors, exhibiting specific capacitances of 291.2 F g^{-1} at 1 A g^{-1} and 240.1 F g^{-1} at 10 A g^{-1}, and exceptional cyclic stability with 93.2% of the capacitance retention over 100,000 cycles. Furthermore, such method is applied to other five bio-wastes, verifying its universality. In addition, the multiple pore-forming mechanism of potassium ferrate is investigated. This work provides a simple and general method to convert abandoned bio-wastes into ideal supercapacitor electrode materials, which holds great potential in energy storage applications.

Keywords: Bio-waste; potassium ferrate; solid-state pyrolysis; hierarchical porous carbon; supercapacitors

1. INTRODUCTION

Batteries and supercapacitors are playing a crucial role in energy storage and conversion applications.[1-5] Long operating life and high power density make supercapacitors an ideal candidate for energy storage devices.[6] As a typical electric

double layer capacitive material, carbon materials have been deeply investigated as electrode materials for supercapacitors,[7] such as activated carbon,[8] carbon nanotubes,[9] carbon aerogels,[10] carbon fibers[11] and graphene.[12,13]

Besides aforementioned carbon materials, biomass carbon has been used in supercapacitors and plays a key role in the development of electrode materials. Biomass carbon is generally prepared by high temperature carbonization using various biomass materials as precursors. For instance, rice bran,[14] coffee beans,[15] popcorn,[16] seaweed,[17] poplar wood,[18] prolifera[19] and sugarcane bagasse[20] have been used as carbon sources to prepare biomass carbon. The synthesis of biomass carbon can not only provide more choices for electrode materials, but also effectively dispose of annoying wastes and protect the environment, which is a good strategy of killing two birds with one stone.

The synthesis of biomass carbon usually includes two steps or even more complicated procedures, such as pre-carbonization, carbonization, activation and so on.[21,22] The complex process, high cost and time-consuming characteristics are the main drawbacks of existing methods. It is necessary to develop a simple, economical and green approach to prepare biomass carbon.

Potassium ferrate is an excellent oxidizing agent, which possesses the efficient disinfection property. Potassium ferrate can be decomposed into potassium hydroxide and ferric hydroxide at high temperatures and both of them contribute to the generation of porous structure.[23] Thus, it is possible to synthesize multi-hierarchical porous carbon by introducing potassium ferrate in solid-state pyrolysis processes.

In this work, waste tea derived porous carbon (WTPC) was synthesized by a simple one-step solid-state pyrolysis method, using potassium ferrate as the pore forming agent. The as-obtained WTPC was used as electrode materials for ultra-long life supercapacitors and its electrochemical properties were evaluated. The as-fabricated supercapacitor yielded a specific capacitance of 291.2 F g^{-1} at 1 A g^{-1}, and prominent cyclic performance with 93.2% of capacitance retention after as long as 100,000 cycles. To explore the universality of this strategy, other five types of biomass waste including shrimp shell, chestnut shell, lamb bone, pomelo peel and peanut shell were used to synthesize porous carbon by the same protocols. This simple, time-saving and green synthetic method provides an ideal choice for the synthesis of biomass carbon, demonstrating a great potential in the disposal of various biomass wastes. This work is a meaningful attempt to recycle bio-wastes and maximize the use of precious natural resources, which is vital for our society with a growing shortage of resources.

2. EXPERIMENTAL

2.1 Preparation of WTPC

The one-step solid-state pyrolysis method was used to synthesize many biomass derived carbon materials, while for simplicity, the synthetic process using waste tea as raw materials was described in detail. Schematic diagram for the synthesis of WTPC is shown in Figure 1. First of all, waste tea was collected and washed to remove undesirable impurities. The above sample was dried and grinded into powder afterwards. Next, 0.5 g of waste tea powder and 3 g of potassium ferrate powder were grinded together for 1 h until they were uniformly mixed. Subsequently, the above

mixture was transferred to a porcelain boat and annealed at 800 ℃ for 1 h under nitrogen protection in a tube furnace. Finally, the product was collected, washed with hydrochloric acid solution and deionized water, and dried at 70 ℃ overnight to obtain WTPC. The same protocols were applied to shrimp shell, chestnut shell, lamb bone, pomelo peel and peanut shell as well. In addition, the controlled experiments without the potassium ferrate were carried out to determine the multiple pore-forming effect of potassium ferrate in the synthetic process.

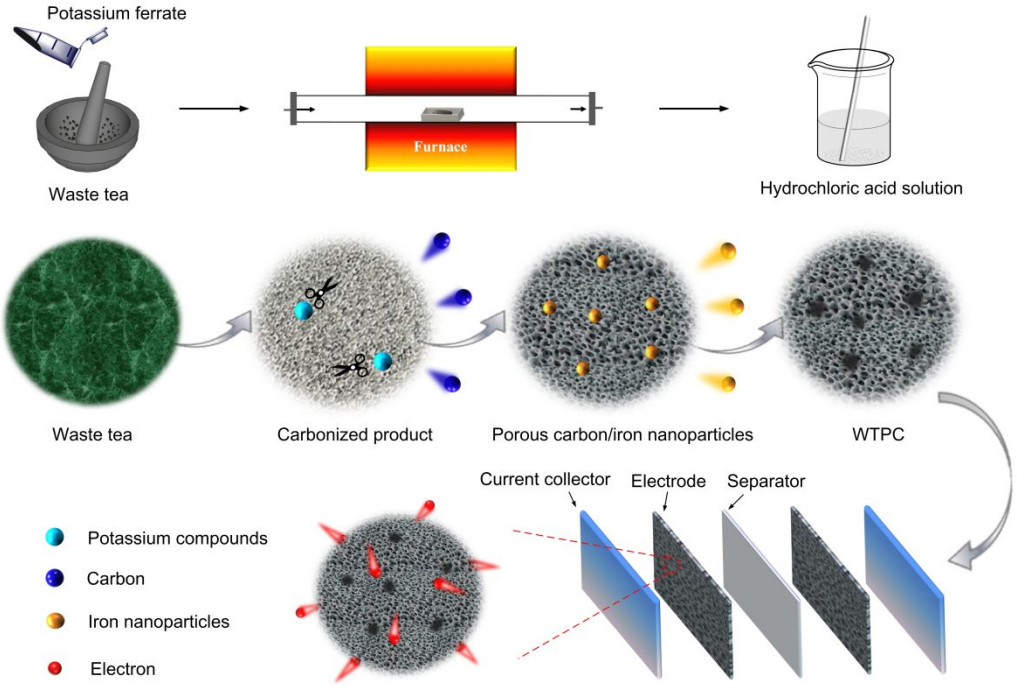

Figure 1 Schematic diagram for the synthesis of WTPC and charge transfer in WTPC electrodes.

2.2 Characterization

Scanning electron microscopy (SEM) was operated with a Nova NanoSEM 450 incorporated with an Energy dispersive spectrometry (EDS). Transmission electron microscopy (TEM) was performed on a FEI TF30 microscope. X-ray diffraction (XRD) was conducted on an X-ray diffractometer (Rigaku MiniFlex 600) with Cu K_{α}

radiation. Nitrogen sorption isotherm was tested by a Micromeritics ASAP 2020 analyzer. Chemical compositions were investigated by X-ray photoelectron spectroscopy (XPS, ESCALAB 250).

2.3 Electrochemical measurement

WTPC and polytetrafluoroethylene (weight ratio of 90: 10) was mixed thoroughly. Anhydrous ethanol was used to disperse the above mixture by sufficient grinding. The resulting paste was coated onto a nickel foam and dried at 80 ℃ for 8 h. The exact weight of active material was determined according to the difference between weights of the bare and coated nickel foam. Cyclic voltammograms (CV, CHI 760E) were recorded in a potential range of -1 to 0 V. Platinum foil and Hg/HgO were employed as counter and reference electrodes, respectively. Electrochemical impedance spectroscopy (EIS, CHI 760E) was conducted with 5 mV amplitude from 100 kHz to 0.1 Hz. Electrochemical tests were accomplished in KOH solution (6 mol/L).

To explore the practical application of the synthesized WTPC, symmetrical supercapacitors with two identical working electrodes were assembled. The charge and discharge characteristics of the assembled device were tested by galvanostatic charge-discharge (GCD, LAND CT2001A). All electrochemical properties including specific capacitances (C_s, F g^{-1}), energy density (E, Wh kg^{-1}) and power density (P, W kg^{-1}) were calculated based on GCD results of the assembled supercapacitors (two-electrode system).

C_s can be calculated by equation (1), and E and P can be obtained from equations

(2) and (3).[24]

$$C_s = 2I\Delta t/m\Delta V \quad (1)$$

$$E = C_s (\Delta V)^2/(4\times3.6) \quad (2)$$

$$P = E/\Delta t \quad (3)$$

where I is the current (A), $\triangle t$ is the discharge time (s), m is the mass of WTPC (g), $\triangle V$ is the potential range (V).

3. RESULTS AND DISCUSSION

Figure 2 shows the structural characterizations of WTPC. SEM images with different magnifications demonstrate the bulk, skeleton structure of pristine waste tea (Figure 2a, b). Figure 2c & d display micro-, meso- and macro-porous structure of the as-obtained WTPC, which shows the typical multi-hierarchical porous structure. Moreover, the detailed micro-structure of WTPC can be verified by the high magnification SEM image in Figure 2e. A large quantity of pores with size of approximately 40 nm can be clearly observed. Figure 2f illustrates the EDS mapping of the as-synthesized WTPC, which only shows carbon and oxygen element, indicating no impurities were introduced into the product. This result is also validated by the XPS spectrum of WTPC in Figure 2k. Morphologies of other five porous carbon materials synthesized by this one-step solid-state pyrolysis method are shown in Figures S1-5.

The multi-hierarchical porous structure was further confirmed by TEM. As shown in Figure 2g, a large number of pores with size of approximately 40 nm can be

observed. These pores increase the interfacial contact area between WTPC and electrolyte and allow rapid diffusion of electrolyte ions, rendering superior ion transport and electrochemical performance. To confirm the multiple pore-forming effect originated from potassium ferrate, controlled experiments without using the potassium ferrate were carried out. SEM and TEM images of the controlled sample are shown in Figure S6, illustrating irregular bulk morphologies and a few pores. There is a big difference between morphologies of WTPC and controlled sample, which confirms the pivotal role of potassium ferrate in the synthetic process.

Two sharp diffraction peaks appear at 26.5° and 43.3° in the XRD pattern of WTPC (Figure 2h), which can be ascribed to the (002) and (100) planes, respectively. The strong intensity and well defined shape of the diffraction peaks reveal good crystalline structure of the as-synthesized WTPC.[25] This result is different from most biomass derived carbon materials reported previously, which show (002) diffraction peaks with weak intensity.[25] To investigate the great effect of potassium ferrate on the structure of carbon, XRD pattern of carbon prepared without using potassium ferrate is shown in Figure S6g (see Electronic Supplementary Material, ESI). The improved crystallinity of WTPC is attributed to the graphitization process at high temperature catalyzed by the iron element, which is derived from the decomposition of potassium ferrate. It is noteworthy that other five porous carbon materials synthesized by the same protocols exhibit similar XRD pattern with strong and well defined (002) diffraction peak, demonstrating the universality of this method.

Figure 2i demonstrates the nitrogen sorption isotherm of WTPC. It is a classical IV

type isotherm, which confirms the existence of mesopores.[19] Furthermore, a high specific surface area (SSA) calculated by the nitrogen adsorption/desorption results is 1671.6 m^2 g^{-1}. Pore size distribution of WTPC is depicted in Figure 2j. Clearly, WTPC manifests a decentralized distribution (<2 nm, ~40 nm and 80 nm). Such large specific surface area and decentralized distribution guarantee fast ion transport and improve capacitive performance.[21,26,27] These pores increase the interfacial contact area between WTPC and electrolyte and allow rapid diffusion of electrolyte ions, rendering superior ion transport and electrochemical performance. Nitrogen sorption isotherm of carbon prepared without using potassium ferrate is shown in Figure S6h (see ESI), and its SSA is only 84.5 m^2 g^{-1}. This result also confirms the multiple pore-forming effect of potassium ferrate in the synthetic process of multi-hierarchical porous carbon. Chemical compositions of WTPC can be obtained from XPS analysis, as shown in Figure 2k. Two photoelectron peaks at 284.5 and 532.0 eV correspond to C1s and O1s respectively,[28] revealing that WTPC consists of C and O element without any impurities. This result concurs with the EDS mapping analysis. Figure S7 shows the Raman spectra of the pristine carbon prepared without using potassium ferrate and WTPC. Two prominent peaks appear at ~1330 and ~1590 cm^{-1}, corresponding to the D and G band, respectively. The ratio of D to G band ($I_{D/G}$) is a powerful indicator of the disorder degree for carbon materials.[25-27] WTPC shows higher $I_{D/G}$ than the pristine carbon, indicating that more structural defects are introduced during the reaction between potassium ferrate and biomass sources.

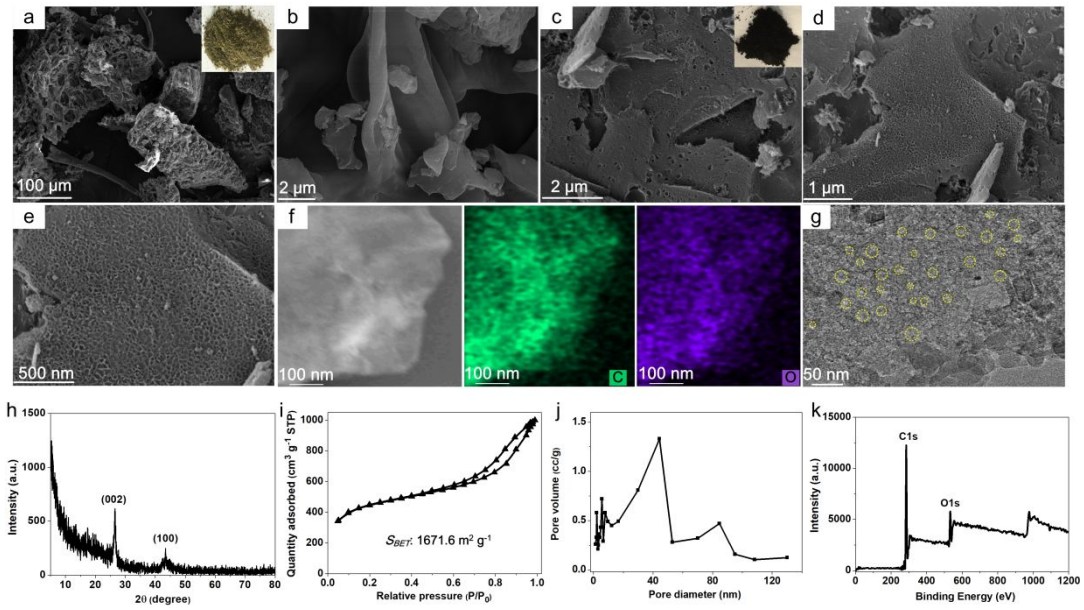

Figure 2 SEM images of waste tea (a, b) and WTPC (c-e); EDS mapping (f), TEM image (g), XRD pattern (h), nitrogen adsorption/desorption isotherm (i), pore size distribution (j) and XPS spectrum (k) of WTPC.

CV curves of the WTPC electrode are displayed in Figure 3a. The quasi-rectangular shape of all four curves indicates electric double layer capacitive (EDLC) behavior.[29] As shown in Figure 3b, the Nyquist plots of the WTPC electrode comprise a sloping line in low-frequency domain and a semicircle in high-frequency domain. Small radius of the semicircle and large slope of the line indicate low charge transfer resistance and diffusive resistance,[26,30,31] thus leading to enhanced electrochemical performances.

Figure 3c shows GCD curves of the assembled symmetrical supercapacitor. The perfect triangular shape with negligible deformation and symmetric characteristics of GCD curves indicate good EDLC behavior,[32] which echoes the CV analysis. Specific capacitances of the symmetrical supercapacitor are calculated based on the GCD

results (Figure 3d). The values are 291.2 F g^{-1} at 1 A g^{-1} and 240.1 F g^{-1} at 10 A g^{-1}, indicating good capacitive properties. As expected, specific capacitances slowly declined with enlarging current density from 0.1 to 10 A g^{-1} (~76% of retention).

The cycling property and Coulombic efficiency of the symmetrical supercapacitor are demonstrated in Figure 3e. Coulombic efficiency is nearly 100% during the whole charge/discharge cycles. The assembled supercapacitor exhibits excellent long-term cyclic property with 93.2% of capacitance retention over 100,000 cycles. To investigate the reason for such outstanding cycling property, SEM of the WTPC electrode after 100,000 cycles is conducted and shown in Figure S8. Clearly, the multi-hierarchical porous structure of WTPC exhibits negligible changes (collapse, blockage, aggregation, etc.), demonstrating its structural integrity and robustness. Such structural characteristics ensure the stable and efficient transport of ions and electrons in long-term cycles, resulting in superior cycling property.

Figure 3f shows the Ragone plots of as-assembled symmetrical supercapacitor. An energy density of 20.2 Wh kg^{-1} can be achieved at a current density of 1 A g^{-1}. Furthermore, a power density is as high as 4919 W kg^{-1} at 10 A g^{-1}, while the energy density is 16.7 Wh kg^{-1}. These results outperform some previously reported carbon based electrode materials.[33-40] A detailed comparison of capacitive performance between our work with previous reports is summarized in Table 1. The detailed capacitive performances of the pristine carbon prepared without using potassium ferrate and WTPC are compared in Figure S9.

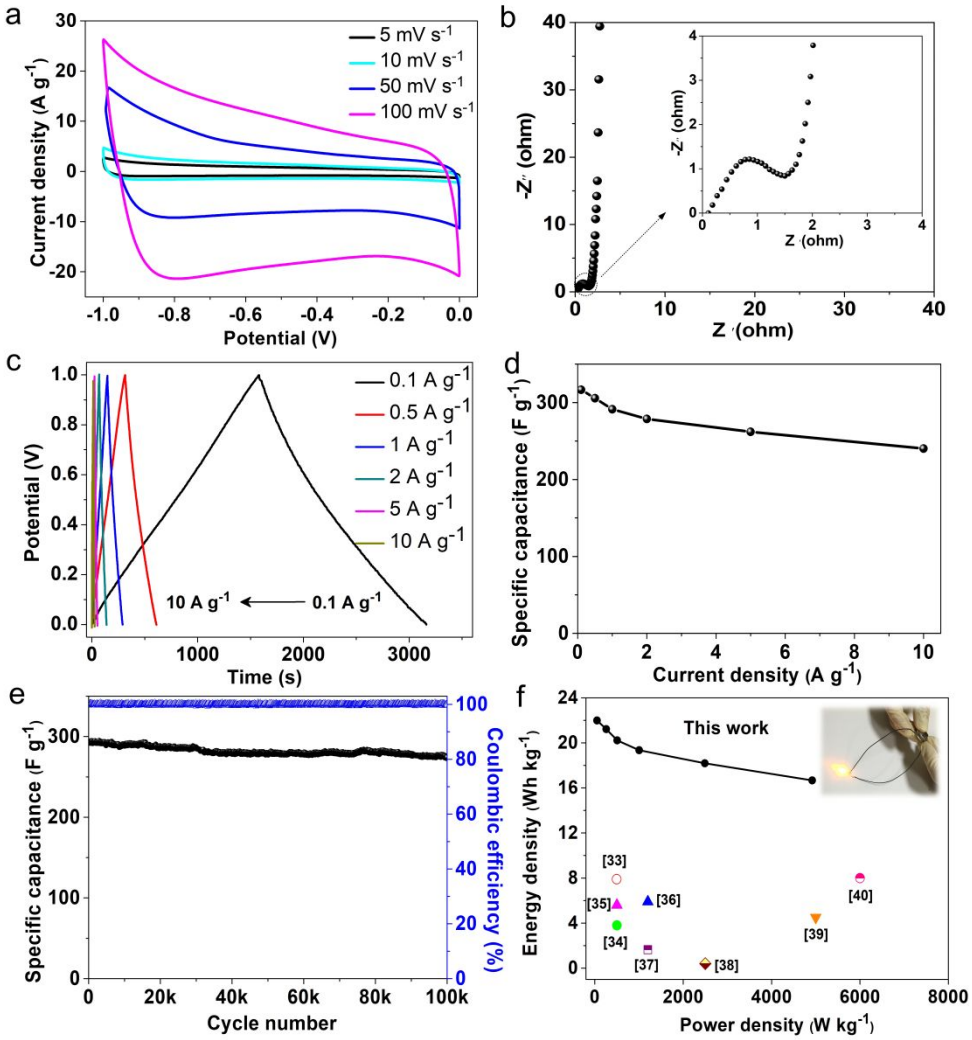

Figure 3 Three-electrode system: CV curves (a) and Nyquist plots (b) of the WTPC electrode; Two-electrode system: GCD curves (c), specific capacitances at different current densities (d), cycling property and Coulombic efficiency at 1 A g^{-1} (e), and Ragone plots (f) of the assembled symmetrical supercapacitors.

Table 1 Summary of capacitive performances for different carbon based supercapacitors

Materials	Energy density (Wh kg^{-1})	Power density (W kg^{-1})	Electrolyte	Reference
3D porous graphitic carbons	7.9	494	KOH	33
Microporous carbon sphere	3.8	500	KOH	34
Hydrogel derived heteroatom doped porous carbon networks	5.6	500	KOH	35
N-doped carbon fibers	5.9	1200	H_3PO_4/PVA	36
Graphene/carbon cloth	1.64	1200	H_2SO_4/PVA	37
Paper coated with CNT	0.4	2500	H_2SO_4/PVA	38
3D graphene hydrogel	4.5	5000	H_2SO_4/PVA	39
Biomass-derived B/N co-doped carbon	8.0	6000	KOH	40
	20.2	**506**		
WTPC	**18.2**	**2490**	**KOH**	**This work**
	16.7	**4919**		

To investigate the generality of this method, various biomass wastes including shrimp shell, chestnut shell, lamb bone, pomelo peel and peanut shell are employed as raw materials to prepare porous carbon by the same strategy. Figures S1-S5 demonstrate the SEM images and XRD patterns of these five kinds of biomass waste derived porous carbon materials, and GCD curves and cyclic performances of the corresponding supercapacitors. The porous carbon materials derived from these biomass wastes exhibit similar structures, demonstrating the universality of this method. Specific capacitances of the porous carbon originated from shrimp shell, chestnut shell, lamb bone, pomelo peel and peanut shell are 234.8, 229.6, 222.8, 216.4 and 209.1 F g^{-1} respectively at 1 A g^{-1}. Moreover, they exhibit excellent cyclic stability over 100,000 cycles, with 93.3%, 89.7%, 90.8%, 88.6% and 98.1% of the

capacitance retention, respectively. These results confirm the generality of this potassium ferrate assisted one-step method in the synthesis of biomass waste derived porous carbon materials.

To shed light on the reason why the as-obtained porous carbon materials exhibit excellent capacitive performance, we investigate the reaction mechanism of potassium ferrate in pore-forming processes and find that potassium ferrate would decompose into potassium hydroxide and ferric hydroxide at high temperatures.[23] On one hand, potassium compounds, which originate from the decomposition of potassium hydroxide at high temperatures, can etch carbon to form carbon dioxide and carbon monoxide, resulting in a porous structure. On the other hand, ferric hydroxide reacts with carbon to form iron particles under an inert atmosphere at high temperatures. The resulting iron particles are removed by the hydrochloric acid solution, leaving massive amounts of pores. EDS, XRD and XPS analysis of the annealed samples before and after washing by hydrochloric acid were carried out, as shown in Figures S10 and S11.

It can be seen from Figure S10a that the annealed sample before washing by hydrochloric acid consists of C, O, K and Fe elements. However, after washing by hydrochloric acid, the final product (WTPC) only contains C and O elements. Simple substances and compounds of K and Fe are removed during the pickling process. XRD pattern of the sample before washing by hydrochloric acid (Figure S10b) indicates the existence of potassium carbonate and iron. As shown in Figure S11b, the WTPC only demonstrates two prominent peaks at 26.5° and 43.3°, corresponding to

(002) and (100) planes of carbon, respectively.[25] This result confirms the removal of potassium compounds and iron after acid pickling process, which can also be proved by XPS results. C, O, K and Fe elements appear in the survey scan XPS spectrum of annealed sample before washing by hydrochloric acid. In the Fe2p high resolution XPS spectrum, a photoelectron peak at 706.7 eV can be attributed to $Fe2p_{3/2}$ of iron.[2,13] However, only C1s and O1s photoelectron peaks appear at 284.5 and 532.0 eV respectively, indicating that WTPC consists of C and O element without any impurities.[28] This result concurs with the EDS mapping analysis.

Since potassium ferrate plays a key role in the pore-forming processes, the effect of potassium ferrate dosage on capacitive performances of the synthesized WTPC has been investigated. In the control experiments, the masses of potassium ferrate are 1 g, 2 g and 4 g, respectively. Accordingly, the as-obtained samples are denoted as WTPC-1, WTPC-2 and WTPC-4, respectively. Figures S12-S14 show GCD, specific capacitance and cyclic property of these three symmetrical supercapacitors. All of them exhibit perfect triangular shape with negligible deformation and symmetric characteristics of GCD curves (Figures S12a, 13a and 14a). Clearly, all WTPC prepared with different potassium ferrate dosages show good EDLC behaviors. Moreover, various WTPC supercapacitors exhibit different specific capacitances at different current densities. The specific capacitance increases with increasing the mass of potassium ferrate from 1 g to 3 g, and remains stable as the mass is further increased to 4 g. Too less potassium ferrate cannot generate enough pores in the product, causing deficient ion transport channels and a slow ion transport

characteristic. However, further increasing the mass of potassium ferrate to 4 g results in a low yield of carbon materials, which is due to the full reaction between potassium ferrate and carbon. In addition, all devices exhibit excellent cyclic property and Coulombic efficiency. There is no noticeable capacitance fading after 10,000 cycles at 1 A g^{-1} for all three devices, as shown in Figures S12c, 13c and 14c.

Reactions associated with potassium ferrate pore-forming process are shown in Figure 4. The multi-hierarchical porous structure and large specific surface area offer an interconnected conductive network, sufficient active surface and short ion diffusion paths for rapid charge transfer and ion diffusion, leading to the superior electrochemical performances.[23] More remarkably, the multi-hierarchical porous structure simultaneously provides excellent ion reservoir, transport and adsorption, avoiding long ion transport distances and large transport resistance, and thus increases the ion transport efficiency.[19]

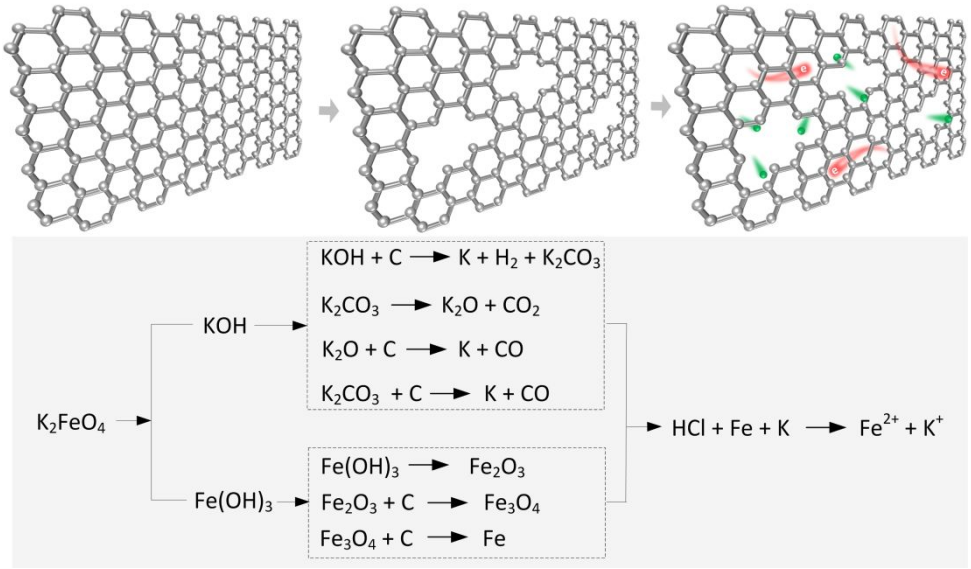

Figure 4 The structural evolution of WTPC and related reactions in the potassium ferrate pore-forming process.

4. CONCLUSIONS

In summary, we developed a simple one-step solid-state pyrolysis method to synthesize multi-hierarchical porous biomass carbon from waste tea. Multiple pore forming effect originated from potassium ferrate resulted in the multi-hierarchical porous structure which led to a specific capacitance of 291.2 F g^{-1} and an energy density of 20.2 Wh kg^{-1} at 1 A g^{-1} for the assembled WTPC based symmetrical supercapacitor. Furthermore, it exhibited a high energy density of 16.7 Wh kg^{-1} at a power density of 4919 W kg^{-1}. In addition, it showed only 6.8% capacitance fading over as long as 100,000 cycles. These outstanding performances made the abandoned waste tea one type of promising precursor for supercapacitor electrode materials. More remarkably, the potassium ferrate assisted one-step solid-state pyrolysis strategy was proved to be a universal method to convert various biomass wastes into porous carbon materials, showing great potentials and bright prospects in the bio-waste recycling and synthesis of biomass derived carbon.

ACKNOWLEDGEMENTS

We thank the Key Research and Development Program of Shandong Province (Grant No. 2019GGX103050), Natural Science Foundation of Shandong Province (Grant Nos. ZR2018BB046, ZR2017BB008), and National Natural Science Foundation of China (Grant No. 21805168, 52003111). W.-Y.W. is grateful to the financial support from the Hong Kong Research Grants Council (PolyU 153051/17P),

Hong Kong Polytechnic University (1-ZE1C), Research Institute for Smart Energy (RISE) and Ms Clarea Au for the Endowed Professorship in Energy (847S). PCQ thanks the Foundation of Wenzhou Science & Technology Bureau (No. W20170003) and the National Natrual Science Foundation of China (No. 21828102).

REFERENCES

1. J. Hwang, S. Myung and Y. Sun, Sodium-ion batteries: present and future, *Chem. Soc. Rev.*, 2017, **46**, 3529-3614.
2. X. Tang, H. Liu, X. Guo, S. Wang, W. Wu, A. K. Mondal, C. Wang and G. Wang, A novel lithium-ion hybrid capacitor based on an aerogel-like MXene wrapped Fe_2O_3 nanosphere anode and a 3D nitrogen sulphur dual-doped porous carbon cathode, *Mater. Chem. Front.*, 2018, **2**, 1811-1821.
3. L. Lyu, K. Seong, D. Ko, J. Choi, C. Lee, T. Hwang, Y. Cho, X. Jin, W. Zhang, H. Pang and Y. Piao, Recent development of biomass-derived carbons and composites as electrode materials for supercapacitors, *Mater. Chem. Front.*, 2019, **3**, 2543-2570.
4. J. Huang, B. Wu, S. Lyu, T. Li, H. Han, D. Li, J. Wang, J. Zhang, X. Lu and D. Sun, Improving the thermal energy storage capability of diatom-based biomass/polyethylene glycol composites phase change materials by artificial culture methods, *Sol. Energ. Mat. Sol. C.*, 2021, **219**, 110797.
5. M. Fu, Z. Zhu, Q. Zhuang, Z. Zhang, W. Chen and Q. Liu, In situ growth of manganese ferrite nanorods on graphene for supercapacitors, *Ceram. Int.*, 2020, **46**, 28200-28205.
6. X. Yang, C. Cheng, Y. Wang, L. Qiu and D. Li, Liquid-Mediated Dense Integration of Graphene Materials for Compact Capacitive Energy Storage, *Science*, 2013, **341**, 534-537.
7. M. Fu, R. Lv, Y. Lei, M. Terrones, Ultra-light flexible electrodes of nitrogen-doped carbon macrotube sponges for high-performance supercapacitors, *Small*, 2020, 10.1002/smll.202004827.
8. J. Y. Hwang, M. Li, M. F. El-Kady and R. B. Kaner, Next-Generation Activated Carbon Supercapacitors: A Simple Step in Electrode Processing Leads to Remarkable Gains in Energy Density, *Adv. Funct. Mater.*, 2017, **27**, 1605745.
9. J. Yu, W. Lu, S. Pei, K. Gong, L. Wang, L. Meng, Y. Huang, J. P. Smith, K. S. Booksh, Q. Li, J. H. Byun, Y. Oh, Y. Yan and T. W. Chou, Omnidirectionally Stretchable High-Performance Supercapacitor Based on Isotropic Buckled Carbon Nanotube Films, *ACS Nano*, 2016, **10**, 5204-5211.
10. C. H. J. Kim, D. Zhao, G. Lee and J. Liu, Strong, Machinable Carbon Aerogels for High Performance Supercapacitors, *Adv. Funct. Mater.*, 2016, **26**, 4976-4983.
11. G. Zhang, Y. Song, H. Zhang, J. Xu, H. Duan and J. Liu, Radially Aligned Porous Carbon Nanotube Arrays on Carbon Fibers: A Hierarchical 3D Carbon Nanostructure for

High-Performance Capacitive Energy Storage, *Adv. Funct. Mater.*, 2016, **26**, 3012-3020.

12. M. Fu, Q. Zhuang, Z. Zhu, Z. Zhang, W. Chen, Q. Liu, H. Yu, Facile synthesis of V2O5/graphene composites as advanced electrode materials in supercapacitors, *J. Alloys Compd*., 2020, 158006.
13. M. Fu, Z. Zhang, Z. Zhu, Q. Zhuang, W. Chen, H. Yu, Q. Liu, Facile synthesis of strontium ferrite nanorods/graphene composites as advanced electrode materials for supercapacitors, *J. Colloid Interface Sci*., 2020, https://doi.org/10.1016/j.jcis.2020.11.114.
14. S. Zhang, H. Gao, J. Li, Y. Huang, A. Alsaedi, T. Hayat, X. Xu and X. Wang, Rice husks as a sustainable silica source for hierarchical flower-like metal silicate architectures assembled into ultrathin nanosheets for adsorption and catalysis, *J. Hazard. Mater.*, 2017, **321**, 92-102.
15. C. Huang, T. Sun and D. Hulicova-Jurcakova, Wide Electrochemical Window of Supercapacitors from Coffee Bean-Derived Phosphorus-Rich Carbons, *Chemsuschem*, 2013, **6**, 2330-2339.
16. T. Liang, C. Chen, X. Li and J. Zhang, Popcorn-Derived Porous Carbon for Energy Storage and CO2 Capture, *Langmuir*, 2016, **32**, 8042-8049.
17. D. Kang, Q. Liu, J. Gu, Y. Su, W. Zhang and D. Zhang, "Egg-Box"-Assisted Fabrication of Porous Carbon with Small Mesopores for High-Rate Electric Double Layer Capacitors, *ACS Nano*, 2015, **9**, 11225-11233.
18. M. Liu, L. Kong, P. Zhang, Y. Luo and L. Kang, Porous wood carbon monolith for high-performance supercapacitors, *Electrochim. Acta*, 2012, **60**, 443-448.
19. J. Cui, Y. Xi, S. Chen, D. Li, X. She, J. Sun, W. Han, D. Yang and S. Guo, Prolifera-Green-Tide as Sustainable Source for Carbonaceous Aerogels with Hierarchical Pore to Achieve Multiple Energy Storage, *Adv. Funct. Mater.*, 2016, **26**, 8487-8495.
20. T. E. Rufford, D. Hulicova-Jurcakova, K. Khosla, Z. Zhu and G. Q. Lu, Microstructure and electrochemical double-layer capacitance of carbon electrodes prepared by zinc chloride activation of sugar cane bagasse, *J. Power Sources*, 2010, **195**, 912-918.
21. M. Fu, W. Chen, X. Zhu, B. Yang and Q. Liu, Crab shell derived multi-hierarchical carbon materials as a typical recycling of waste for high performance supercapacitors, *Carbon*, 2019, **141**, 748-757.
22. M. Fu, Z. Zhu, Z. Zhang, Q. Zhuang, W. Chen and Q. Liu, Microwave deposition synthesis of Ni(OH)2/sorghum stalk biomass carbon electrode materials for supercapacitors, *J. Alloys Compd.*, 2020, **846**, 156376.
23. Y. Gong, D. Li, C. Luo, Q. Fu and C. Pan, Highly porous graphitic biomass carbon as advanced electrode materials for supercapacitors, *Green Chem.*, 2017, **19**, 4132-4140.
24. F. Zhang, T. Zhang, X. Yang, L. Zhang, K. Leng, Y. Huang and Y. Chen, A high-performance supercapacitor-battery hybrid energy storage device based on graphene-enhanced electrode materials with ultrahigh energy density, *Energ. Environ. Sci.*, 2013, **6**, 1623-1632.
25. L. Chen, Y. Zhang, C. Lin, W. Yang, Y. Meng, Y. Guo, M. Li and D. Xiao, Hierarchically porous nitrogen-rich carbon derived from wheat straw as an ultra-high-rate anode for lithium ion batteries, *J. Mater. Chem. A*, 2014, **2**, 9684-9690.
26. F. Wu, J. Gao, X. Zhai, M. Xie, Y. Sun, H. Kang, Q. Tian and H. Qiu, Hierarchical porous carbon microrods derived from albizia flowers for high performance supercapacitors, *Carbon*, 2019, **147**, 242-251.
27. H. Jin, X. Feng, J. Li, M. Li, Y. Xia, Y. Yuan, C. Yang, B. Dai, Z. Lin, J. Wang, J. Lu and S. Wang,

Heteroatom-Doped Porous Carbon Materials with Unprecedented High Volumetric Capacitive Performance, *Angew. Chem. Int. Edit.*, 2019, **58**, 2397-2401.

28. M. Fu, Z. Zhu, W. Chen, H. Yu and Q. Liu, Microwave assisted synthesis of MoS2/graphene composites for supercapacitors *J. Mater. Sci.*, 2020, **55**, 16385-16393.
29. Poonam, K. Sharma, A. Arora and S. K. Tripathi, Review of supercapacitors: Materials and devices, *J. Energy Storage*, 2019, **21**, 801-825.
30. J. Wang, Y. Cui and D. Wang, Design of Hollow Nanostructures for Energy Storage, Conversion and Production, *Adv. Mater.*, 2019, **31**, 1801993
31. S. Yun, Y. Zhang, Q. Xu, J. Liu and Y. Qin, Recent advance in new-generation integrated devices for energy harvesting and storage, *Nano Energy*, 2019, **60**, 600-619.
32. Y. Liu, J. Xu, X. Gao, Y. Sun, J. Lv, S. Shen, L. Chen and S. Wang, Freestanding transparent metallic network based ultrathin, foldable and designable supercapacitors, *Energ. Environ. Sci.*, 2017, **10**, 2534-2543.
33. F. Ma, D. Ma, G. Wu, W. Geng, J. Shao, S. Song, J. Wan and J. Qiu, Construction of 3D nanostructure hierarchical porous graphitic carbons by charge-induced self-assembly and nanocrystal-assisted catalytic graphitization for supercapacitors, *Chem. Commun.*, 2016, **52**, 6673-6676.
34. Z. Li, D. Wu, Y. Liang, R. Fu and K. Matyjaszewski, Synthesis of Well-Defined Microporous Carbons by Molecular-Scale Templating with Polyhedral Oligomeric Silsesquioxane Moieties, *J. Am. Chem. Soc.*, 2014, **136**, 4805-4808.
35. B. You, F. Kang, P. Yin and Q. Zhang, Hydrogel-derived heteroatom-doped porous carbon networks for supercapacitor and electrocatalytic oxygen reduction, *Carbon*, 2016, **103**, 9-15.
36. Y. Cheng, L. Huang, X. Xiao, B. Yao, L. Yuan, T. Li, Z. Hu, B. Wang, J. Wan and J. Zhou, Flexible and cross-linked N-doped carbon nanofiber network for high performance freestanding supercapacitor electrode, *Nano Energy*, 2015, **15**, 66-74.
37. S. Wang, B. Pei, X. Zhao and R. A. W. Dryfe, Highly porous graphene on carbon cloth as advanced electrodes for flexible all-solid-state supercapacitors, *Nano Energy*, 2013, **2**, 530-536.
38. Y. J. Kang, H. Chung, C.-H. Han and W. Kim, All-solid-state flexible supercapacitors based on papers coated with carbon nanotubes and ionic-liquid-based gel electrolytes, *Nanotechnology*, 2012, **23**, 065401.
39. Y. Xu, Z. Lin, X. Huang, Y. Liu, Y. Huang and X. Duan, Flexible Solid-State Supercapacitors Based on Three-Dimensional Graphene Hydrogel Films, *ACS Nano*, 2013, **7**, 4042-4049.
40. Z. Ling, Z. Wang, M. Zhang, C. Yu, G. Wang, Y. Dong, S. Liu, Y. Wang and J. Qiu, Sustainable Synthesis and Assembly of Biomass-Derived B/N Co-Doped Carbon Nanosheets with Ultrahigh Aspect Ratio for High-Performance Supercapacitors, *Adv. Funct. Mater.*, 2016, **26**, 111-119.

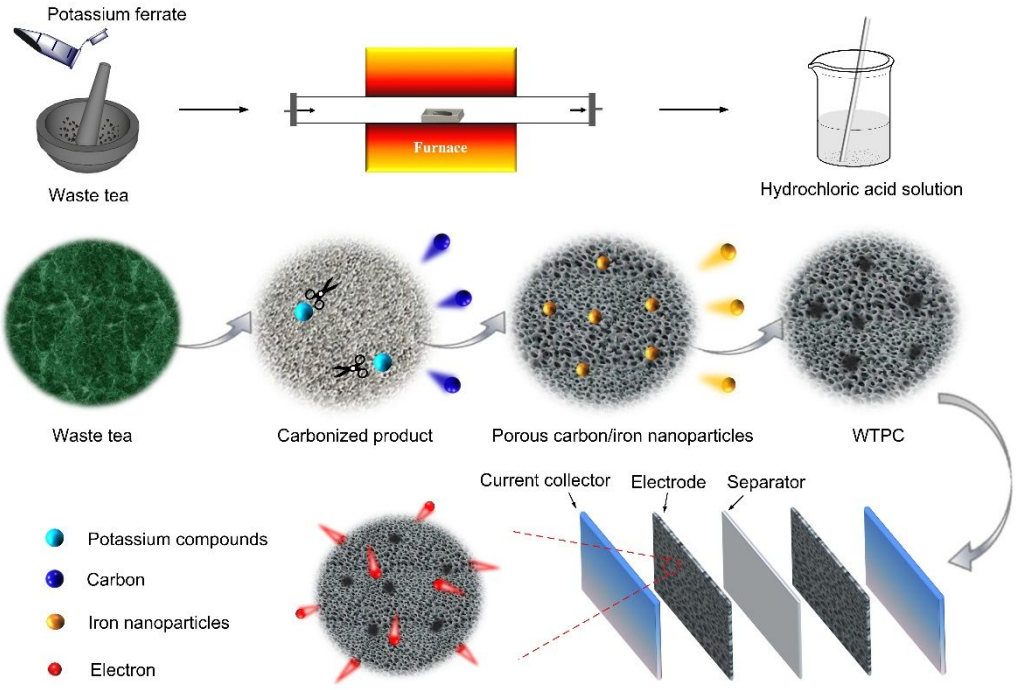

Kill two birds with one stone: recycling wastes to synthesize ultra-long life supercapacitor electrode materials is developed by a general one-step solid-state pyrolysis method.